BETTER UNDERSTANDING OF THE BIOLOGICAL EFFECTS OF RADIATION BY MICROSCOPIC APPROACHES

EUN-HEE KIM
Department of Nuclear Engineering, Seoul National University
599 Gwanak-ro, Gwanak-gu, Seoul 151-744, Korea
E-mail : eunhee@snu.ac.kr

Received November 30, 2008

Radiation has stochastic aspects in its generation, its choice of interaction mode during traveling in media, and its impact on living bodies. In certain circumstances, like in high dose environments resulting from low-LET radiation, the variance in its impact on a target volume is negligible. On the contrary, in low dose environments, especially when they are attributed to high-LET radiation, the impact on the target carries with it a large variance. This variation is more significant for smaller target volumes. Microdosimetric techniques, which have been developed to estimate the distribution of radiation energy deposited to cellular and subcellular-sized targets, contrast with macrodosimetric techniques which count only the average value. Since cells and DNA compounds are the critical targets in human bodies, microdosimetry, or dose estimation by microscopic approach, helps one better analyze the biological effects of radiation on the human body. By utilizing microbeam systems designed for individual cell irradiation, scientists have discovered that human cells exhibit radio-sensitive reactions without being hit themselves (bystander effect). During the past 10 or more years, a new therapeutic protocol using discontinuous multiple micro-slit beams has been investigated for its clinical application. It has been suggested that the beneficial bystander effect is the essence of this protocol.

KEYWORDS : Microdosimetry, Microbeam, Individual Cell Irradiation, Radiation Therapy

1. INTRODUCTION

Radiation has the potential to cause many changes in the human body. When it is used for medical purposes, the process of exposing the human body to radiation is cautiously designed to obtain the best results from it. In therapeutic applications, the ultimate goal is to deliver enough energy to disable the target cells and at the same time with no harmful effects on the non-targeted cells. The diagnostic exposure, on the other hand, shall be taken at the lowest dose level on the condition that useful information is obtainable. The "lowest dose level" is expected not to cause any short-term physical harm to the patient.

Whether there exists a dose level below which the human body is totally safe from radiation damage has been debated for the past few decades. The "Low Dose Radiation Research Program", operated by U.S. DOE since 1999, and the "EU Framework Program, Theme: Radiation Protection" are the major systems that support research activities on the biological effects of low-dose radiation. In fact, some of these studies date back to mid 1960s. The field of "microdosimetry" was derived from attempts to ascertain "real" energy deposition phenomenon in micron-sized volumes typical of human cells, especially in low dose environments. Kellerer [1] and Rossi [2] established the bases of the theoretical and experimental methodologies, respectively. In microdosimetric approaches, the stochastic variation of energy deposition in small targets is presented in the form of probabilistic density function of specific quantity.

The microbeam cell-irradiation system was invented to simulate the low beam-intensity radiation impinging on micron-sized targets. The system was devised in 1990 by Braby and Reece [3] at Pacific Northwest National Laboratory (PNNL). Their idea was embodied by Braby himself at PNNL [4], Randers-Pehrson et al. at Columbia University [5], and Folkard et al. at the Gray Cancer Institute (GCI) [6-8] up to the late 1990s. At present, there are 10 or more microbeam systems worldwide including ones built in Germany [9], France [10], Japan [11] and Korea [12].

The conceptual basis of radiation therapy utilizing discontinuous beam patterns lies in the fact that the threshold dose for complications resulting from radiation treatment increases as the irradiated volume of tissues is reduced [13]. Its beneficial aspect, in terms of an increased *therapeutic ratio*, was observed in animal studies as early as 1961 [14]. The current microbeam radiation therapy (MRT) protocol utilizing a microplanar beam of synchrotron

X-rays was initiated by Slatkin et al [15]. Through animal studies [16,17], the MRT protocol has proved promising for the treatment of brain tumors, especially in children.

This paper emphasizes improvements in the understanding of the interaction of radiation with biological substances, namely cells and DNA compounds, and their responses. These improvements were made by switching the scale, in which the radiation phenomena are experimented and analyzed, from the macroscopic (millimeter and larger) range to the microscopic (micrometer and nanometer) range.

2. DOSE ESTIMATION FOR MICRO- AND NANO-SCALE TARGETS

When radiation interacts with matter, multiple outcomes are possible. For example, a photon entering a medium may be absorbed resulting in the emission of fluorescence X-rays or Auger electrons (photoelectric absorption). The photon may emerge deflected from its original trajectory and with reduced energy (Compton scattering). Photon absorption can also result in the emission of multiple photons (pair production) or in the initiation of nucleus splitting. It is not possible to predict which event occurs at each step of a cascade of interactions with complete certainty, but it is possible to predict which events are more likely to happen. Monte Carlo simulation codes can reflect theses probabilistic aspects inherent in the interactions of radiation with matter.

Microdosimetry studies were pursued to give a more realistic description of energy deposition to micron-sized targets exposed to low doses of radiation. Experimental studies along these same lines have been advanced by the development of Rossi-type proportional counters (Rossi counters). The Rossi counter, named after its inventor, is a spherical chamber with a tissue-equivalent wall and a tissue-equivalent filler gas. In a mixed radiation field, one can measure the spectra of lineal energy by utilizing a Rossi counter. If a single spectrum is split up into partial spectra, one can distinguish the low-, medium-, and high-LET fractions of the total dose [18]. Among the most recently developed instruments is a proportional counter that can simulate a 1 mm-diameter target. Nose

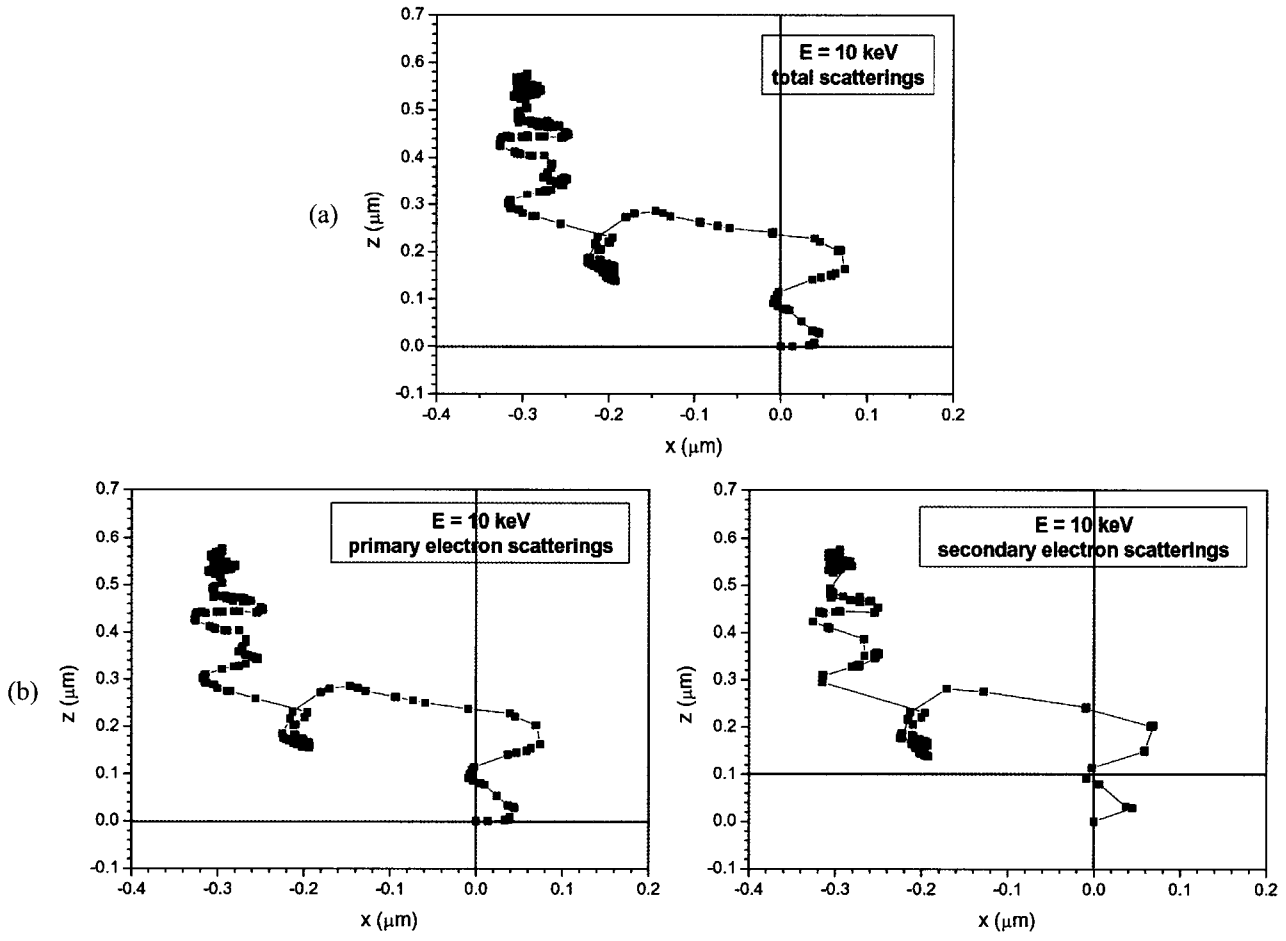

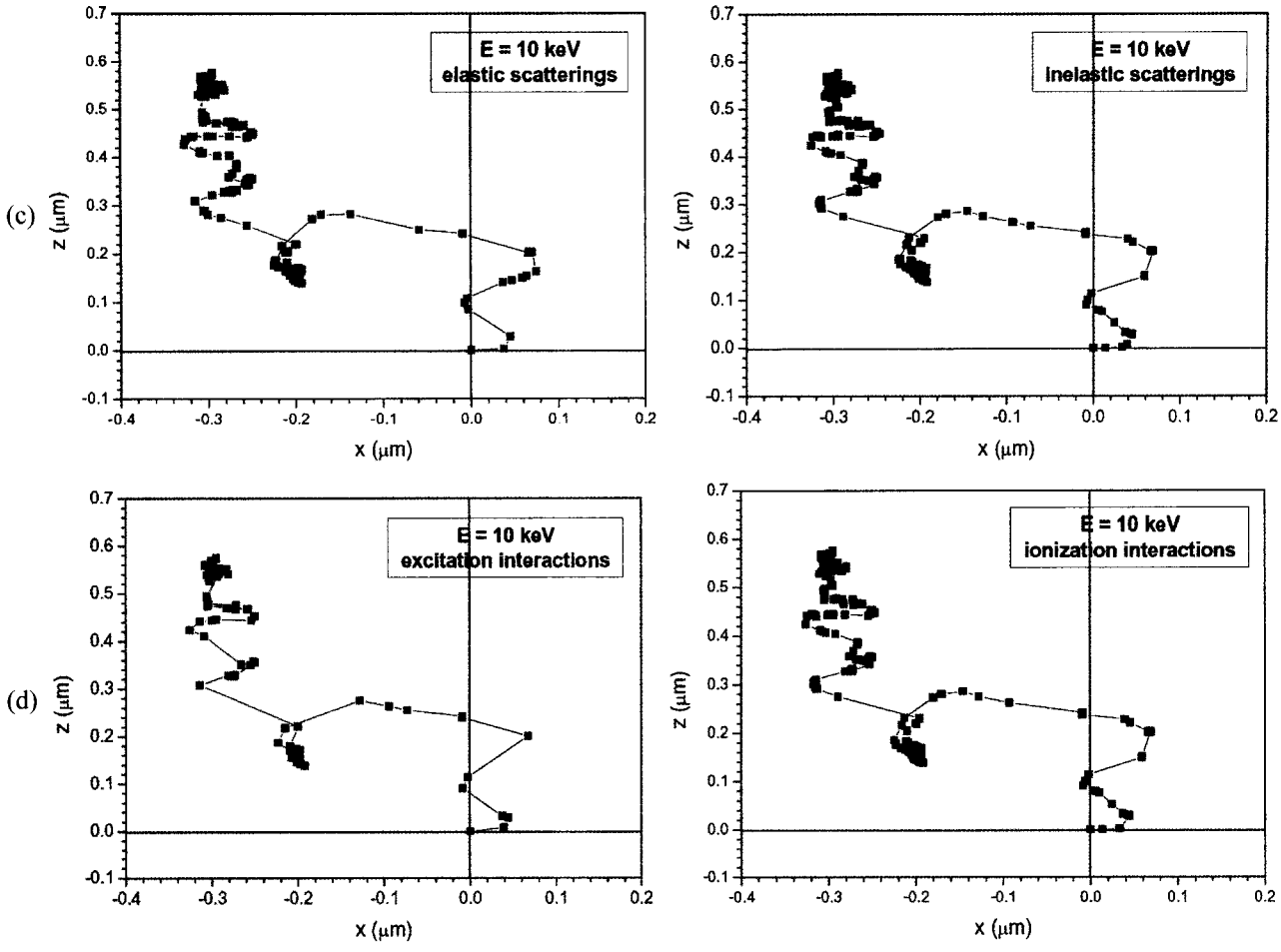

Fig. 1. 10 Tracks (View on X-Z Plane) in Liquid Water Drawn by a 10 keV Electron Eemitted at Origin and in the Positive X-Direction: (a) a Total Track, (b) Primary and Secondary Electron Tracks, (c) Elastic and Inelastic Scattering Tracks, and (d) Excitation and Ionization Event Tracks

et al. [19] developed this proportional counter to measure the impact of heavy ions. Rayadurgam [20] also developed one that enables simulation of targets down to10 nm in size.

Electrons are at the final step in local energy deposition regardless of the primary radiation type. Therefore, accurate cross sections of tissue-equivalent matter for the interactions of electrons, especially at low energy, are essential for giving a realistic description of energy deposition to small targets. Theoretical analyses of energy deposition in micron-sized targets were preceded by preparations of the cross section data for electrons interacting with a *liquid* water medium as opposed to a gaseous medium. In the early period, inelastic cross sections were calculated by taking plasmon excitation into account [21]. In a later version of inelastic cross sections [22], which were further improved [23], plasmon excitation was excluded from the inelastic scattering modes in agreement with Lavern and Mozumber [24].

OREC [25], CPA100 [26], and the ETMICRO-ETCHEM program package [27,28] are some of the many Monte Carlo codes that have been written for simulating electron transport and their associated interactions in liquid water. OREC was revised to NOREC [29] by having its original elastic scattering cross sections replaced by National Institute of Standards and Technology (NIST) data. In all of these programs, electrons are traced down to around 10 eV, which allows one to obtain the energy deposition record in detail, even for nanometer-sized targets.

The ETMICRO-CHEM package consists of E_PHYS, PRECHEM and CHEM modules. The inelastic scattering cross sections included in the E_PHYS module were calculated on the basis of the Emfietzoglou-Nikjoo model [22]. The elastic scattering cross sections originate

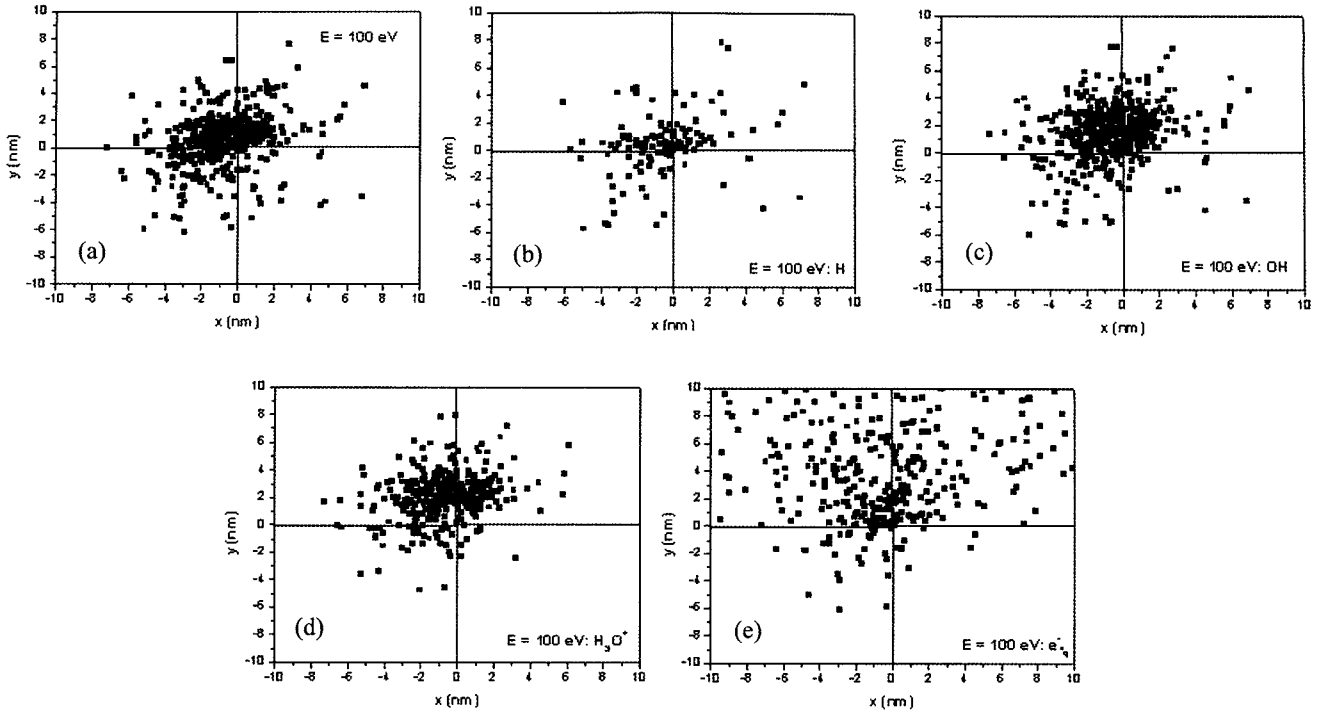

Fig. 2. The Spatial Distributions of Radicals for a Single 100 eV-electron Emission at Origin and in the Positive X-direction: (a) Locations of Ionization and Excitation Events at the Physical Stage, and (b-e) Spatial Distributions of H, OH, H_3O^+ and e^-_{aq} Radicals, respectively, at the End of Prechemical Stage

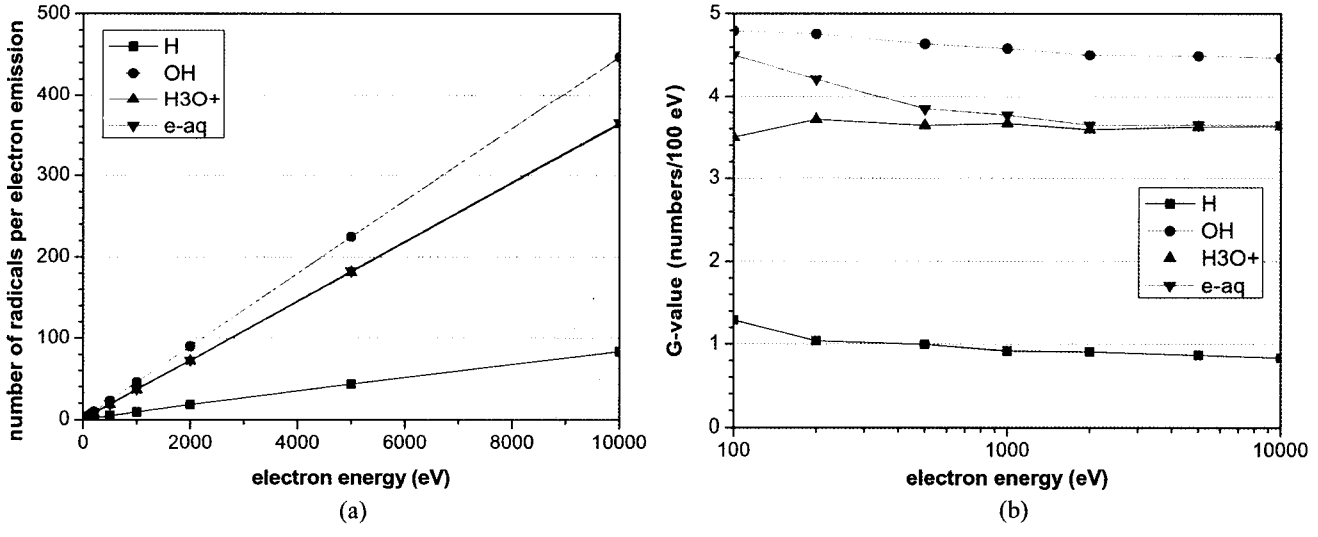

Fig. 3. The Production of Radicals H, OH, H_3O^+ and e^-_{aq} by the Primary Electron Emissions at 100 eV to 10 keV: (a) the Numbers of Radicals at the Beginning of Chemical Stage and (b) the Corresponding G-values

from various research outcomes [30-32]. The electron tracing cut-off is set at 10 eV in kinetic energy, whereas the tracing upper limit is 10 keV. E_PHYS provides the spatial distribution of electron and water-molecule interactions identifying whether the electrons are primary or secondary, whether the interaction is elastic or inelastic scattering, and in the case of inelastic scattering whether water molecules are excited or ionized (see Fig 1). The

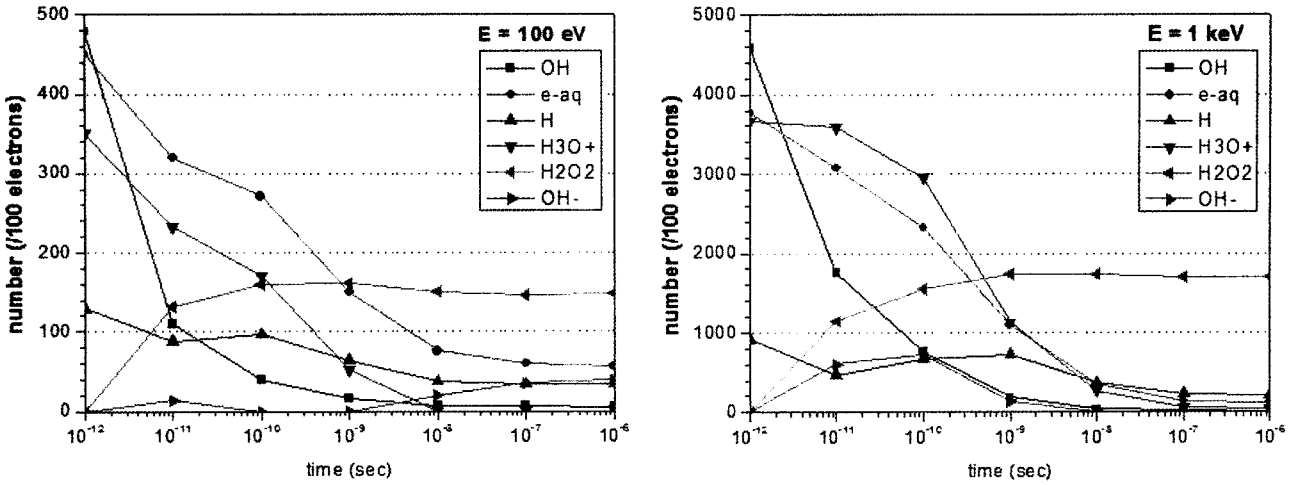

Fig. 4. Radical Population as a Function of Time in the Chemical Stage ($10^{-12} \sim 10^{-6}$ sec): (a) for 100 eV Electrons and (b) for 1 keV Electrons

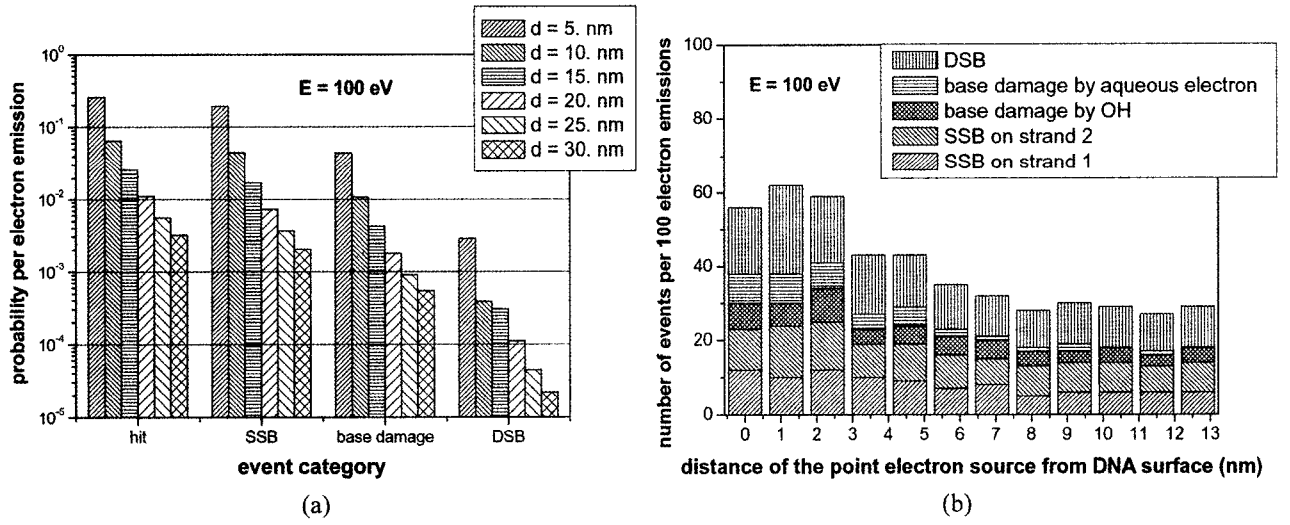

Fig. 5. DNA Damage by 100 eV Electrons for Different Source Distances from DNA Surface: (a) by Direct Action and (b) by Indirect Action

primary chemical products H_2O^+, H_2O^*, and the sub-excitation electron e^-_{sub} from ionizations and excitations of water molecules are further traced in the PRECHEM and CHEM modules, which cover the prechemical and chemical interactions, respectively. It is thought that the prechemical stage starts at ~1 fs (10^{-15} sec) and the chemical stage starts at ~1 ps (10^{-12} sec) from the point of initial electron emission.

Excitation and ionization events identified at the physical stage (Fig 2(a)) result in the production of radicals H, OH, H_3O^+ and e^-_{aq} (Fig 2 (b-e)) through the prechemical stage. Populations of the radicals vary depending on the initial energy of electron emission as informed in Fig 3. In the beginning of chemical stage, radicals H, OH, H_3O^+ and e^-_{aq} interact with each other leading to the production of other radicals H_2O_2 and OH^-. The spatial distributions of radicals H, OH, H_3O^+, e^-_{aq}, H_2O_2 and OH^- are controlled by both the diffusion coefficients of each radical species and the reaction radii for each reactant pair. Radical populations as a function

of time are shown in Fig 4. Rate constants for different chemical combinations and effective reaction radii have been adopted from various sources [33-35].

With the ETMICRO-CHEM program package, one can also estimate DNA damage caused by direct and indirect actions of electrons. The estimates given in Fig 5 were made for the DNA volume model of Nikjoo et al [36]. Assumptions took for the calculation were as follows: the threshold energy of 17.5 eV applies to both single strand break and base damage during direct actions; for indirect action, base damage is caused only by OH and e^-_{aq}; and sugar backbone breaks are caused only by the attack of OH radicals. The double strand break was counted when a couple of single strand breaks occurred within a 10-base pair distance.

3. EXPERIMENTS UTILIZING INDIVIDUAL CELL IRRADIATION SYSTEM

Since Braby and Reece suggested that a system enabling individual-cell targeting ("microbeam system") would help one observe what really happens to irradiated cells, there have been more than 10 microbeam systems built in the world. Two in particular, one at Columbia University in USA [5] and another one at GCI in UK [6,7] have contributed to the majority of research achievements involving individual cell-targeting experiments. In both systems, alpha particles played the main role as the primary radiation.

The most significant finding from the microbeam studies is the "bystander effect," whereby the cells neighboring radiation-hit cells are influenced [37-39]. Mechanisms behind the bystander effect include gap-junction intercellular communication and factor secretion from the hit cells. The gap-junction communication between cells in contact was strongly backed up by the work of Zhou et al [40,41]. In their experiments, cells pretreated with lindane or octanol, which inhibits gap junction-mediated intercellular communication, showed a significant reduction in mutant yield. They also observed that the radical scavenger DMSO had no effect on the mutagenic incidence. Morgan, on the other hand, asserted that there is a factor secreted from the hit cells that can stimulate the un-irradiated cells and this factor must be both soluble and capable of being transported through the cell-to-cell gap junction communication channels [42]. He further proved the bystander effect *in vivo* [43]. Blood plasma isolated from individuals who had been exposed to ionizing radiation caused chromosomal aberrations in blood lymphocytes from non-irradiated individuals after coculture. It became even more evident through the work of Mothersill and Seymour that the factor secreted by the irradiated cell is responsible for the bystander effect [44]. Un-irradiated cells showed a significant fall in cloning efficiency after receiving medium from the irradiated culture in the presence of cells, whereas no effect was observed from the un-irradiated cells that had received medium from the irradiated culture in the absence of cells.

By taking advantage of the microbeam system, one can not only hit the target cells exclusively, but also deliver a selected number of charged particles to each target. Miller et al. observed that the oncogenicity of exactly one alpha particle was significantly lower than that of a Poisson-distributed mean of one alpha particle [45], which implies that oncogenic risk is attributed mostly to the cells traversed by multiple alpha particles. Assuming that this applies in general, one can conjecture that the risk from low-level exposure to alpha particles may be overestimated by extrapolation from a high-level dose risk.

At GCI, an X-ray microbeam is also available [8]. Studies on individual-cell irradiation with electron microbeams have been performed at Texas A&M University, at PNNL, and at Korea Institute of Radiological and Medical Sciences (KIRAMS) [12]. Sowa et al. at PNNL demonstrated micronucleus formation in human diploid fibroblasts by delivering an electron pulse beam at low energies (25 keV and 80 keV) [46]. The electron beam was more effective at lower energies in inducing the micronucleus formation. This supports the hypothesis that electrons at track end are mainly responsible for the biological damage to the cells.

4. THERAPEUTIC ADVANTAGES OF SPACIAL BEAM FRACTIONATION

MRT studies first began at the National Synchrotron Light Source (NSLS) facility, Brookhaven National Laboratory (BNL) in USA [15] and later at the European Synchrotron Radiation Facility (ESRF) in Grenoble, France [47]. Synchrotron radiation beams appropriate for MRT are also available at the SPring8 site in Japan [48]. The operational specifications arranged for MRT studies at these three synchrotron facilities are listed in Table 1. The range of the synchrotron X-ray beam energy lies between 100 and 140 keV [48-50], and the maximum electron beam current in the storage ring ranges from 100 to 300 *mA*. X-ray energy determines not only the maximum treatment depth but also the minimum center-to-center distance between nearby micron-sized slits allowed for saving the radiation-blocked tissue volume. Maximum electron beam current determines the maximum X-ray beam intensity that can be extracted from the synchrotron. Higher beam intensities allow shorter exposure times for a given dose.

The beam collimators at NSLS, ESRF, and Spring8 are all slightly different in design. The multi-slit collimator (MSC) at the Spring8 site has thirty slits of dimensions 25 μm in height, 30 mm in width, and 5 mm in depth separated with a spacing of 200 μm [48]. An

Table 1. Main Parameters of Three Major Synchrotrons in Use for MRT Studies

Site		Collimator	Electron Energy (GeV)	Maximum Current (mA)	Median X-ray Energy (keV)
France	European Synchrotron Radiation Facility in Grenoble	Multi-slit micro-collimator	6	200	107
USA	National Synchrotron Light Source at Brookhaven National Laboratory	Interlaced micro-collimator	2.8	300	120
Japan	SPring-8 at Japan Synchrotron Radiation Research Institute	Multi-slit micro-collimator	8	100	139

alternating stack of 175 μm-thick tungsten plates and 25 μm-thick polyimide sheets makes up the MSC. The tungsten plate attenuates the majority of energy fluence, whereas the polyimide sheet transmits the majority of photon energy. The gas-cooled multi-slit collimator at ESRF is assembled with two identical 8 mm-thick tungsten blocks [51]. An interlaced X-ray microplanar beam is available at NSLS [52]. These collimators have common functionality: the 20 to 90 μm-wide openings allow X-rays to reach the target volume and deliver "peak doses", while the 100 to 300 μm-wide alternating blocked volumes are saved by the delivery of "valley doses". The goal of MRT studies is to improve therapeutic effects by inducing a greater "peak-to-valley dose ratio" under the condition that valley doses are maintained below the normal tissue tolerance dose.

Animal studies using microplanar X-ray beams have produced a few interesting results. First, normal tissues, including the central nervous system, can tolerate doses of up to several hundreds of Gy (typical tolerance dose for broad beam irradiation is ~20 Gy) [53]. Second, the brain sparing effect in the MRT protocol seems to depend mostly on the valley dose and little on the peak dose [54]. The sparing effect vanishes only when the valley dose approaches the tissue tolerance dose for broad beams. Third, the biological process underlying normal-tissue sparing may involve rapid regeneration of the tissue's microvessels by the capillary endothelial cells that survived at the radiation-blocked tissue volume [55].

Grid radiation therapy also adopts spatially fractionated radiation beams. Grid therapy, however, differs from the MRT protocol in several aspects. First, it is a palliative treatment rather than a therapeutic treatment [56]. Second, the beam diameter and the center-to-center distance of the neighboring grid beams are of the order of centimeters [57]. Third, typical beam energies in grid therapy are of the order of mega electron-volts; typical MRT beam energies are of the order of kilo electron-volts [58]. In addition, beams of choice in grid therapy include both electron and photon beams [59], whereas MRT uses hard X-rays only. Finally, the single dose in grid therapy is up to 20 Gy [57], whereas MRT doses are up to 600 Gy.

5. SUMMARY

Microdosimetry techniques enable one to measure energy deposition in microscopic volumes. As compared to macrodosimetry, a conventional method that provides a single average value of energy deposition, microdosimetry allows one to track the detailed history of radiation events in cellular and subcellular targets thus providing a distribution of possible values. The spread of this distribution is narrow at high doses, but wide at low doses. The effects of low-dose radiation on cellular targets have been of interest in the field of radiation protection. Microdosimetry and microbeam cell-irradiation systems have played significant roles in advancing the knowledge of the low-dose radiation effect on biological units for the past 40 years or more.

Microbeam radiation therapy (MRT) differs from current radiation treatment protocols in that the beam collimator has multiple, discontinuous, micron-sized slits instead of the single millimeter- or centimeter-scale broad-beam. The merits of MRT as a therapeutic protocol have been proven through a number of animal studies. The tolerance dose of normal brain tissue increases from

some tens of Gy for the broad beam irradiation to some hundreds of Gy at microbeam irradiation. The latter brings with it higher therapeutic ratios. The "beneficial bystander effect" may explain the normal tissue sparing observed in MRT [50]: the endothelial cells of the normal tissue vasculature survive at valley-dose exposure and repair the losses to the neighboring endothelial cells at peak-dose exposure.

ACKNOWLEDGMENTS

The author attributes her research achievement partly mentioned in this article, including the ETMICRO-CHEM program and the electron microbeam cell-irradiation system at KIRAMS, and the progress in preliminary study on microbeam radiation therapy to the financial support from the Korea Ministry of Education, Science and Technology under the Nuclear R&D Program.

REFERENCES

[1] A. M. Kellerer and D. Chemelevsky, "Concepts of Microdosimetry: I. Quantities," *Rad. Environ. Biophys.*, **12**, 61 (1975).

[2] L. J. Goodman and H. H. Rossi "The Measurement of Dose Equivalents Using Paired Ionization Chambers," *Health Phys.*, **14**, 168 (1968).

[3] L. A. Braby and W. D. Reece, "Studying Low Dose Effects Using Single Particle Microbeam Irradiation," *Radiat. Prot. Dosim.*, **31**, 311 (1990).

[4] L. A. Braby, "Microbeam Studies of the Sensitivity of Structures within Living Cells," PNL-SA-19443, Pacific Northwest national Laboratory (1991).

[5] G. Randers-Pehrson, C. R. Geard, G. Johnson, C. Elliston and D. Brenner, "The Columbia University Single-Ion Microbeam," *Radiat. Res.*, **156**, 210 (2001).

[6] M. Folkard, B. Vojnovic, K. M. Prise, A. G. Bowey, R. J. Locke, G. Schettino and B. D. Michael, "A Charged-Particle Microbeam: I. Development of an Experimental System for Targeting Cells Individually with Counted Particles," *Int. J. Radiat. Biol.* **72**, 375 (1997).

[7] M. Folkard, B. Vojnovic, K. J. Hollis, A. G. Bowey, S. J. Watts, G. Schettino, K. M. Prise and B. D. Michael, "A Charged-Particle Microbeam: II. A Single-Particle Micro-Collimation and Detection System," *Int. J. Radiat. Biol.*, **72**, 387 (1997).

[8] M. Folkard, G. Schettino, B. Vojnovic, S. Gilchrist, A. G. Michette, S. J. Pfauntsch, K. M. Prise and B. D. Michael, "A Focused Ultrasoft X-ray Microbeam for Targeting Cells Individually with Submicrometer Accuracy," *Radiat. Res.* **156**, 796 (2001).

[9] K.-D. Greif, H. J. Brede, D. Frankenberg and U. Giesen, "The PTB Single Ion Microbeam for Irradiation of Living Cells," *Nucl. Instrum. Meth. Phys. Res. Sec. B: Beam Inter. Mater. At.*, **217**, 505 (2003).

[10] S. Incerti, P. Barberet, R. Villeneuve, P. Aguer, E. Gontier, C. Michelet-Habchi, P. Moretto, D. T. Nguyen, T. Pouthier and R. W. Smith, "Simulation of Cellular Irradiation with the CENBG Microbeam Line Using GEANT4," *IEEE Trans. Nucl. Sci.*, **51**, 1395 (2004).

[11] Y. Kobayashi, T. Funayama, S. Wada, Y. Furusawa, M. Aoki, C. Shao, Y. Yokota, T. Sakashita, Y. Matsumoto, T. Kakizaki and N. Hamada, "Microbeams of Heavy Charged Particles," *Biol. Sci. Space*, **18**, 235 (2004).

[12] E. H. Kim, G. M. Sun and M. Jang, "An Electron Microbeam Cell-Irradiation System at KIRAMS: Performance and Preliminary Experiments," *Radiat. Prot. Dosim.*, **122**, 297 (2006).

[13] H. R. Withers, J. M. G. Taylor and B. Maciejewski, "Treatment Volume and Tissue Tolerance," *Int. J. Radiat. Oncol. Biol. Phys.*, **14**, 751 (1988).

[14] W. Zeman, H. J. Curtis and C. P. Baker, "Histopathologic Effect of High-Energy-Particle on the Visual Cortex of the Mouse Brain," *Rad. Res.*, **15**, 496 (1961).

[15] D. N. Slatkin, P. Spanne, F. A. Dilmanian and M. Sandborg, "Microbeam Radiation Therapy," *Med. Phys.*, **19**, 1395 (1992).

[16] D. N. Slatkin, P. Spanne, F. A. Dilmanian, J. –O. Gebbers and J. A. Laissue, "Subacute Neuropathological Effects of Microplanar Beams of X-rays from a Synchrotron Wiggler," *Proc. Natl. Acad. Sci. USA*, **92**, 8783 (1995).

[17] J. A. Laissue, G. Geiser, P. O. Spanne, F. A. Dilmanian, J. O. Gebbers, M. Geiser, X. Y. Wu, M. S. Makar, P. L. Micca, M. M. Nawrock, D. D. Joel and D. N. Slatkin, "Neuropathology of Ablation of Rat Gliosarcomas and Contiguous Brain Tissues Using a Microplanar Beam of Synchrotron-Wiggler-Generated X Rays, *Int. J. Cancer*, **78**, 654 (1998).

[18] J. B. Leroux and Y. Herbaut, "Rossi Counter Measurements in Mixed Fields," *Radiat. Prot. Dosim.*, **9**, 227 (1984).

[19] H. Nose, N. Matsufuji, Y. Kase and T. Kanai, "Biological Dose Distribution Analysis with Microdosimetry: Experiment and Monte Carlo Simulation," *Proc. Nucl. Sci. Symp.*, Honolulu, USA, Oct. 26-Nov. 3, 2007.

[20] S. Rayadurgam, "Design of a Wall-Less Proportional Counter for Microdosimetry in Nanometer Dimensions," M.S. Thesis, Texas A&M University (2005).

[21] M. Dingfelder, D. Hantke, M. Inokuti and H. G. Paretzke, "Electron Inelastic-Scattering Cross Sections in Liquid Water," *Radiat. Phys. Chem.*, **53**, 1 (1999).

[22] D. Emfietzoglou and H. Nikjoo, "The Effect of Model Approximations on Single-Collision Distributions of Low-Energy Electrons in Liquid Water," *Radiat. Res.*, **163**, 98 (2005).

[23] D. Emfietzoglou and H. Nikjoo, "Accurate Electron Inelastic Cross Sections and Stopping Powers for Liquid Water over the 0.1-10 keV Range Based on an Improved Dielectric Description of the Bethe Surface," *Radiat. Res.*, **167**, 110 (2007).

[24] J. A. LaVerne and A. Mozumder, "Concerning Plasmon Excitation in Liquid Water," *Radiat.Res.*, **133**, 282 (1993).

[25] J. E. Turner, R. N. Hamma, M. L. Souleyrette, D. E. Martz, T. A. Rhea and D. W. Schmidt, "Calculations for Beta Dosimetry Using Monte Carlo Code (OREC) for Electron Transport in Water," *Health Phys.*, **55**, 741 (1988).

[26] M. Terrissol and A. Beaudre, "Simulation of Space and Time Evolution of Radiolytic Species Induced by Electrons in Water," *Radiat. Prot. Dosim.*, **31**, 175 (1990).

[27] E. H. Kim, "Electron Track Simulation Using ETMICRO," *Radiat. Prot. Dosim.*, **122**, 53 (2006).

[28] E. H. Kim, "A New Monte Carlo code ETMICRO-CHEM for Simulating DNA Damage by Electrons," *Proc. 13th Int. Cong. Radiat. Res.*, San Francisco, USA, Jul. 8-12, 2007.

[29] V. A. Semenenko, J. E. Turner and T. B. Borak, "NOREC, a Monte Carlo Code for Simulating Electron Tracks in Liquid Water," *Radiat. Environ. Biophys.*, **42**, 213 (2003).
[30] A.Danjo and H. Nishimura, "Elastic Scattering of Electrons from H_2O Molecule," *J. Phys. Soc. Jap.*, **54**, 1224 (1985).
[31] A. Katase, K. Ishibachi, Y. Matsumoto, T. Sakae, S. Maezono, E. Murakami, K. Watanabe and H. Maki, "Elastic Scattering of Electrons by Water Molecules over the Range 100–1000 eV *J. Phys. B: At. Mol. Phys.*, **19**, 2715 (1986).
[32] B. Grosswednt and E. Waibel, "Transport of Low Energy Electrons in Nitrogen and Gas," *Nucl. Instrum. Meth.*, **155**, 145 (1978).
[33] S. M. Pimblott, "Investigation of Various Factors Influencing the Effect of Scavengers on the Radiation Chemistry Following the High-Energy Electron Radiolysis of Water," *J. Phys. Chem.* **96**, 4485 (1992).
[34] A. J. Elliot, D. R. McCracken, G. V. Buxton and N. D. Wood, "Estimation of Rate Constants for Near-Diffusion-Controlled Reactions in Water at High Temperatures," *J. Chem. Soc. Faraday Trans.*, **86**, 1539 (1990).
[35] G. V. Buxton, C. L. Greenstock, W. P. Helman, A. B. Ross, and W. Tsang, "Critical Review of Rate Constants for Reactions of Hydrated Electrons," *J. Phys. Chem. Ref. Data*, **17**, 513 (1988).
[36] H. Nikjoo, D. E. Charlton, and D. T. Goodhead, "Monte Carlo Track Structure Studies of Energy Deposition and Calculation of Initial DSB and RBE," *Adv. Space Res.*, **14**, 161 (1994).
[37] S. G. Sawant, G. Randers-Pehrson, C. R. Geard, D. J. Brenner and E. J. Hall, "The Bystander Effect in Radiation Oncogenesis: I. Transformation in C3H 10T½ Cells *In Vitro* can be Initiated in the Unirradiated Neighbors of Irradiated Cells," *Radiat. Res.*, **155**, 397 (2001).
[38] S. G. Sawant, G. Randers-Pehrson, N. F. Metting, and E. J. Hall, "Adaptive Response and the Bystander Effect Induced by Radiation in C3H 10T½ Cells in Culture," *Radiat. Res.*, **156**, 177 (2001).
[39] S. G. Sawant, W. Zheng, K. M. Hopkins, G. Randers-Pehrson, H. B. Lieberman and E. J. Hall, "The Radiation-Induced Bystander Effect for Clonogenic Survival," *Radiat. Res.*, **157**, 361 (2002).
[40] H. Zhou, G. Randers-Pehrson, C. A. Waldren, D. Vannais, E. J. Hall and T. K. Hei, "Induction of a Bystander Mutagenic Effect of Alpha Particles in Mammalian Cells", *Proc. Natl. Acad. Sci.*, **97**, 2099 (2000).
[41] H. Zhou, M. Suzuki, G. Randers-Pehrson, D. Vannais, G. Chen, J. E. Trosko, C. A. Waldren, and T. K. Hei, "Radiation Risk to Low Fluences of α Particles May Be Greater than We Thought", *Proc. Natl. Acad. Sci.*, **98**, 14410 (2001).
[42] W. Morgan, "Is There a Common Mechanism Underlying Genomic Instability, Bystander Effects and Other Nontargeted Effects of Exposure to Ionizing Radiation?" *Oncogene*, **22**, 7094 (2003).
[43] W. Morgan, "Non-targeted and Delayed Effects of Exposure to Ionizing Radiation: II. Radiation-Induced Genomic Instability and Bystander Effects *In Vivo*, Clastogenic Factors and Transgenerational Effects," *Radiat. Res.*, **159**, 581 (2003).
[44] C. Mothersill and C. Seymour, "Medium from Irradiated Human Epithelial Cells but not Human Fibroblasts Reduces the Clonogenic Survival of Unirradiated Cells," *Int. J. Radiat. Biol.*, **71**, 421 (1997).
[45] R. C. Miller, G. Randers-Pehrson, C. R. Geard, E. J. Hall and D. J. Brenner, "The Oncogenic Transforming Potential of the Passage of Single α Particles through Mammalian Cell Nuclei," *Proc. Natl. Acad. Sci.*, **96**, 19 (1999).
[46] M. B. Sowa, M. K. Murphy, J. H. Miller, J. C. McDonald, D. J. Strom and G. A. Kimmel, "A Variable-Energy Electron Microbeam: A Unique Modality for Targeted Low-LET Radiation," *Radiat. Res.*, **164**, 695 (2005).
[47] M. Renier, T. Brochard, C. Nemoz and W. Thomlinson, "White-Beam Fast-Shutter for Microbeam Radiation Therapy at the ESRF," *Nucl. Instrum Meth. Phys. Res. A*, 479, 656 (2002).
[48] M. Torikoshi, Y. Ohno, N. Yagi, K. Umetani and Y. Furusawa, "Dosimetry for a Microbeam Array Generated by Synchrotron Radiation at Spring8," *Eur. J. Radiol.*, **68**, 114 (2008).
[49] E. A. Siegbahn, J. Stepanek, E. Brauer-Krisch and A. Bravin, Determination of Dosimetric al quantities used in Microbeam Radiation therapy (MRT) with Monte Carlo Simulations," *Am. Assoc. Phys. Med.*, **33**, 3248 (2006).
[50] F. A. Dilmanian and Y. Qu, "Tissue-Sparing Effect of X-ray Microplanar Beams Particularly in the CNS: Is a Bystander Effect Involved?" *Exp. Hematol.*, **35**, 69 (2007).
[51] E. Brauer-Krisch, A. Bravin, L. Zhang and E. Siegbahn, "Characterization of a Tungsten/Gas Multislit Collimator for Microbeam Radiation Therapy at the European Synchrotron Radiation Facility," *Rev. Sci. Instrum.*, **76**, 64303 (2005).
[52] F. A. Dilmanian, Z. Zhong, T. Bacarian, H. Benveniste, P. Romanelli, R. Wang, J. Welwart, T. Yuasa, E. M. Rosen and D. Anschel, "Interlaced X-ray Microplanar Beams: A Radiosurgery Approach with Clinical Potential," *Proc. Natl. Acad. Space*, **103**, 9709 (2006).
[53] P. Regnard, G. Le Duc, E. Brauer-Krisch, I. Tropres, E. A. Siegbahn, A. Kurak, C. Clair, H. Bernard, D. Dallery, J. A. Laissue and A. Bravin, "Irradiation of Intracerebral 9L Gliosarcoma by a Single Array of Microplanar X-Ray Beams from a Synchrotron: Balance between Curing and Sparing," *Phys. Med. Biol.*, **53**, 861 (2008).
[54] F. A. Dilmanian, T. M. Button, G. Le Duc, N. Zhong, L. A. Pena, J. A. L. Smith, S. R. Martinez, T. Bacarian, J. Tammam, B. Ren, P. M. Farmer, J. Kalef-Ezra, P. L. Micca, M. M. Nawrocky, J. A. Niederer, F. P. Recksiek, A. Fuchs and E. M. Rosen, "Response of Rat Intracranial 9L Gliosarcoma to Microbeam Radiation Therapy," *Neuro. Oncol.*, **4**, 26 (2002).
[55] F. A. Dilmanian, Y. Q. S. Liu, C. D. Cool, J. Gilbert, J. F. Hainfeld, C. A. Kruse, J. Laterra, D. Lenihan, M. M. Nawrocky, G. Pappas, C. I. Szc, T. Yuasa, N. Zhong, Z. Zhong and J. W. McDonald, "X-ray Microbeams: Tumor Therapy and Central Nervous System Research," *Nucl. Instrum. Meth. Phys. Res. A.*, **548**, 30 (2005).
[56] M. Mohiuddin, J. H. Stevens, J. E. Reiff, M. S. Huq and N. Suntharalingam, "Spatially Fractionated (GRID) Radiation for Palliative Treatment of Advanced Cancer," *Radiat. Oncol. Invest.*, **4**, 41 (2007).
[57] R. Zwicker, A. Meigooni and M. Mohiuddin, "Therapeutic Advantage of Grid Irradiation for Large Single Fractions," *Int. J. Radiat. Oncol. Biol. Phys.*, **58**, 1309 (2004).
[58] J. E. Reiff, M. S. Hug, M. Mohiuddin and N. Suntharalingam,

"Dosimetric Properties of Megavoltage Grid Therapy," *Int. J. Radiat. Oncol. Biol. Phys.*, **33**, 937 (2004).
[59] A. S. Meigooni, S. A. Parker, J. Zheng, K. J. Kalbaugh, W. F. Regine and M. Mohiuddin, "Dosimetric Characteristics with Spatial Fractionation Using Electron Grid Therapy," *Med. Dosim.*, **27**, 37 (2002).